

New orientationally ordered phases of a homopolymer

Yu. A. Kuznetsov, E. G. Timoshenko, and K. A. Dawson

Advanced Computational Research and Theory Groups, Centre for Soft Condensed Matter and Biomaterials, Department of Chemistry, University College Dublin, Dublin 4, Ireland

(Received 12 July 1995; accepted 29 September 1995)

We present results of Monte Carlo simulations of a homopolymer with three-body interactions on a lattice. At equilibrium we find three collapsed phases with different orientational order. The first one may be described as a conventional phase with effective three-body attraction. Two other phases are observed in the region of the phase diagram corresponding to three-body repulsion. The second phase is characterized by local orientational order within the globule. The third one possesses global orientational order and it appears to be analogous to nematic phase of a liquid crystal. Kinetics of the collapse transition to the phase III is crucially different from that of phase I and II due to formation of clusters with different orientations at the intermediate stage. This is the origin of a metastable long-lived state in kinetics. © 1996 American Institute of Physics.

[S0021-9606(96)51901-3]

I. INTRODUCTION

There have been various studies recently of the collapse transition of homopolymers.¹⁻³ These studies have focused on both equilibrium and kinetics, mainly for the case where pair interactions are attractive and the collapsed state is stabilized by excluded volume interactions. In this paper we address a somewhat different question. Thus, we consider the consequence on collapse of having a very stiff polymer where neighboring links have a strong preference to adopt locally linear configurations, but the pairwise interaction for more distant segments becomes sufficiently attractive to force collapse. Of course we expect no real changes in the Flory coil since for a fluctuating state only the effective Kuhn length will be modified. However, in the compacted "collapsed" state such polymer chain-contour fluctuations are quenched, and there will be a strong preference for rod-like structure, though of course the single rigid rod is destabilized with respect to the collapsed state.

Finally, before our presentation it is worth mentioning some potential problems with our choice of technique to study this issue. First, the simulation times required for good studies are so long that one prefers to use a lattice model. On the other hand, especially where contour fluctuations are quenched, the lattice structure will fairly strongly affect the results. In particular, when, as we find, orientational symmetry is broken in the globule it may be broken only in three lattice dimensions. There are then two possibilities. First, the continuous model could also have such a broken symmetry, and the error introduced by the lattice is simply that overall globule rotational motions are lost. Alternatively, the discrete nature of the underlying lattice could produce some artefacts. We will discuss this possibility briefly in the final section.

These, then, are the issues that lead us to investigate the model with two- and three-body interactions described in the next section.

Finally, we note that the model we study might well be appropriate to the collapse kinetics of stiff polymers such as DNA, under the action of amphiphilics,⁴ or even the water

soluble polymer poly-*N*-isopropylacrylamide.⁵

II. MODEL

We begin by noting that a previous paper³ contains a complete description of our simulations and model. The only addition here is that we have now included a three-body term. This permits us to have attractive two-body interactions in competition with repulsive three-body interactions, and we focus our discussions on the new features presented by these effects.

The monomer-solvent interaction is now described by the Hamiltonian,

$$H = \frac{1}{2} \sum_{i \neq j} w(r_{ij}) \mathcal{T}_{s_i s_j} + \frac{1}{6} \sum_{i \neq j \neq k} v(r_{ij}, r_{jk}, r_{ik}) \mathcal{T}_{s_i s_j s_k}, \quad (1)$$

where i, j, k numerate lattice sites; s_i labels the state of the site i (monomer m or solvent s), \mathcal{T}_{ab} and \mathcal{T}_{abc} are a 2×2 and $2 \times 2 \times 2$ symmetric tensors of two- and three-body interaction constants, $r_{ij} = |\mathbf{r}_i - \mathbf{r}_j|$, and $w(r)$ and $v(r, r', r'')$ are functions representing the form of the two- and three-body potential interactions. We chose the interaction functions $w(r)$ and $v(r, r', r'')$ so that the range of the three-body interaction is shorter than the range of two-body interaction, namely,⁶

$$w(r) = \begin{cases} 1 & r \leq 2 \\ 0 & r > 2 \end{cases},$$
$$v(r, r', r'') = \begin{cases} 1 & r, r', r'' \leq \sqrt{2} \\ 0 & r, r', r'' > \sqrt{2} \end{cases}.$$

We have used the Metropolis algorithm⁷ for calculation of the transition probability of the system at temperature T . It can be shown that the probability of an update in the system configuration may be expressed as an exponent of a linear combination of two- and three-body interaction parameters. These are defined as follows,

$$\chi^{(2)} \equiv \frac{2\mathcal{I}_{ms} - \mathcal{I}_{mm} - \mathcal{I}_{ss}}{k_B T},$$

$$\chi^{(3)} \equiv \frac{2\mathcal{I}_{mms} - \mathcal{I}_{mmm} - \mathcal{I}_{mss}}{k_B T}, \quad (2)$$

$$\chi^{(3)'} \equiv \frac{2\mathcal{I}_{mss} - \mathcal{I}_{mms} - \mathcal{I}_{sss}}{k_B T}.$$

For simplicity we restrict ourselves by the additional condition $\mathcal{I}_{sab}=0$, which leads to $\chi^{(3)'}=0$. Positive or negative values of the interaction parameters in (2) correspond to attraction or repulsion respectively. Thus, we have only two parameters, those given in Eq. (2), that determine the thermodynamical properties of the system defined by Hamiltonian (1).

One other crucial distinction is incorporated in this work; the use of reptation sampling as well as simple local Metropolis. Thus, because we study the collapsed states we expend some effort to use reptation moves to fully sample the structures. Typically this involves about 10^7 moves for the collapsed ensemble, and we make the normal checks to ensure that very extensive changes in individual configurations are accepted, but the averages remain stable. Therefore, we argue that the collapsed states discussed here are certainly metastable, and almost certainly globally stable.

III. EQUILIBRIUM PROPERTIES

We aim to demonstrate in this section that the phase diagram of the model appears to contain more phases than it is usually expected. We are apparently able to distinguish three different collapsed phases divided by sharp peaks in the heat capacity. These may be characterized by differing degrees of orientational order of the polymer segments.

The phase diagram of the model described by the Hamiltonian (1) is exhibited in Fig. 1. The lower left part of the diagram corresponds to the good solvent conditions and there the Flory coil is preferred. Other regions labeled I, II, and III correspond to compacted globule phases of different types.

In Fig. 2 we exhibit examples of particular polymer configurations representative of these phases. In phase I [see Fig. 2(a)] the packing is space isotropic and it is determined only by connectivity and excluded volume restrictions. The conformation does not possess any order along the chain. This is what is conventionally called the collapsed phase. We prefer to call it the isotropic phase since there are other collapsed phases.

In phase III [see Fig. 2(c)] a typical conformation possesses a preferred direction. Most chain segments are aligned along this direction forming rods that are arranged in a two-dimensional chess-board pattern in the plane perpendicular to the rods. One can see that such a structure minimizes the three-body interaction term of the energy. This phase may be considered analogous to the uniaxial nematic phase of a liquid crystal.⁸ At first this conclusion may seem somewhat surprising because originally the coil does not consist of any elongated objects. However the appearance of rodlike seg-

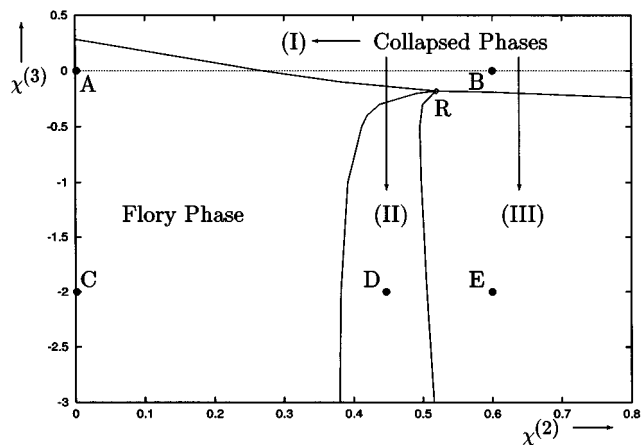


FIG. 1. Phase diagram for homopolymer with degree of polymerization $N=120$. Solid lines correspond to the peaks in the heat capacity, which determine the transition values of the interaction parameters $\chi^{(2)}$ and $\chi^{(3)}$ defined in Eq. (2). Region I of the phase diagram corresponds to isotropic liquid compacted state. Region III corresponds to anisotropic collapsed state, which is analogous to nematic state of liquid crystal. In the region II the single globule consists of several locally ordered regions. The point R appears to represent the joining of all transition curves. However, given the limited numerical accuracy of a Monte Carlo scheme we cannot be certain that they do indeed join.

ments clearly arises because the three-body repulsion makes long straight pieces of chain more favorable, while the two-body effects cause compaction. We should note also, that the radius of gyration in the region I is somewhat smaller than in the region III.

The phase II [see Fig. 2(b)] lies between the Flory phase and orientationally ordered phase III. Again this state is stable because of the balance between long-range two-body attraction and short-range effective three-body repulsion. A typical conformation here consists of locally ordered domains of segments of the chain aligned in different directions. Thus, there is no overall alignment between domains and the phase is globally isotropic.

To make our discussion more formal, let us introduce the orientational order parameters. We denote by $l_r^{(i)}$ the number of consecutive linearly ordered monomer beads along one of the axes, i (x , y , or z). We take into account only rods for which $l_r^{(i)} > 2$. The number of rods per polymer chain along the i axis we denote as $n_r^{(i)}$. Now consider the following quantities,

$$m_r^{(i)} \equiv l_r^{(i)} n_r^{(i)},$$

$$m_r \equiv m_r^{(x)} + m_r^{(y)} + m_r^{(z)}. \quad (3)$$

These give the number of monomers that are aligned along the appropriate directions and their sum. Obviously, space isotropy implies

$$\langle m_r^{(x)} \rangle = \langle m_r^{(y)} \rangle = \langle m_r^{(z)} \rangle. \quad (4)$$

When this isotropy is broken then the values of the three averages are different. In our case there is no explicitly symmetry breaking term in the Hamiltonian (1), analogous to the introduction of an infinitesimal magnetic field in Ising

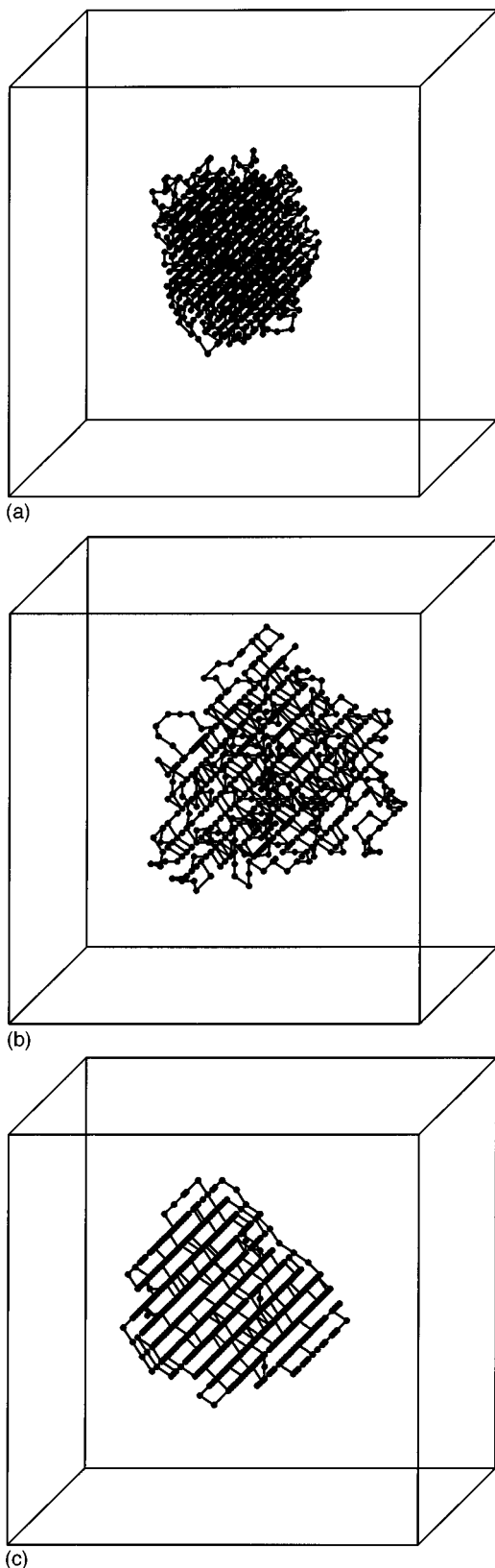


FIG. 2. Equilibrium collapsed polymer configurations for degree of polymerization $N=768$. The size of the framing box is equal to $L=32$. Pictures (a), (b), and (c) corresponds respectively to states found in the regions of the phase diagram labeled by (I), (II), and (III).

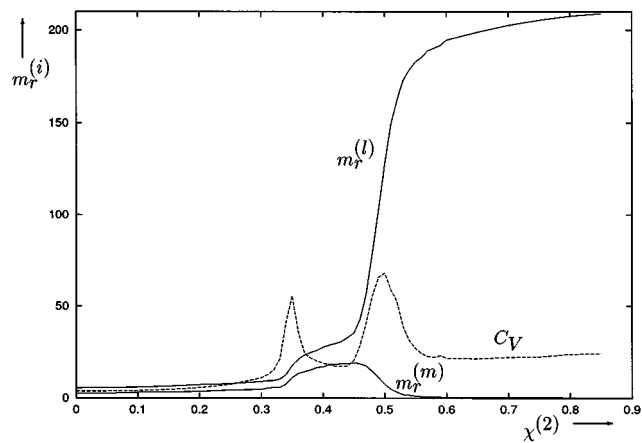


FIG. 3. Plot of $\langle m_r^{(i,m)} \rangle$ vs the two-body interaction parameter $\chi^{(2)}$ for polymer with the degree of polymerization $N=240$ and value of the three-body interaction parameter $\chi^{(3)}=-2$ (locus between C and E in Fig. 1). The plot of heat capacity is labeled by C_V .

model. Thus, we use different observables to distinguish orientational ordering. Let us instead consider the triple $m_r^{(l)}$, $m_r^{(m)}$, and $m_r^{(s)}$, these being respectively the largest, middle and smallest values of the components $m_r^{(i)}$ defined before the statistical averaging.

The behavior of the quantities $\langle m_r^{(l,m,s)} \rangle$ across different lines of the phase diagram (Fig. 1) are shown in Figs. 3 and 4. Simulations show that the dependence of the quantity m_r on the degree of polymerization in the Flory coil state may be well described by a linear law,

$$\langle m_r \rangle = bN, \quad b = 0.0348 + 0.0006, \quad \chi^{(2)} = \chi^{(3)} = 0. \quad (5)$$

The value of the coefficient b is close to that obtained by approximating the excluded volume effect for only the first two nearest neighbors along the chain,⁹

$$b = \frac{1}{91} \sum_{n=0}^{\infty} \frac{3+n}{21^n} \approx 0.035186. \quad (6)$$

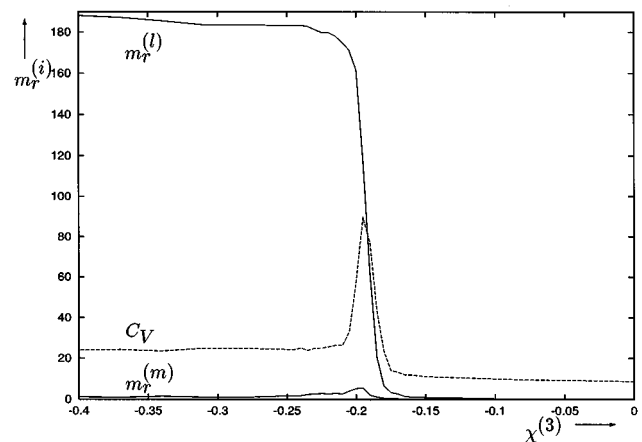


FIG. 4. Plot of $\langle m_r^{(i,m)} \rangle$ vs the three-body interaction parameter $\chi^{(3)}$ for polymer with degree of polymerization $N=240$ and value of the two-body interaction parameter $\chi^{(2)}=0.6$ (locus between B and E in Fig. 1). The plot of heat capacity is labeled by C_V .

TABLE I. Numerical values of parameters α , τ_S , Z , $R_g^2(\infty)$, A_1 , τ_1 from formulas (8)–(10) for polymers of different degree of polymerization N . Exponent α has been obtained by a fitting procedure for times (Ref. 10) up to 0.5×10^3 MCS.

N , line	α	Z	τ_S , 10^3 MCS	$R_g^2(\infty)$	A_1	τ_1 , 10^3 MCS
120, CD	0.66 ± 0.02	0.46 ± 0.03	28	15.6	92	5.4
120, CE	0.65 ± 0.04	0.26 ± 0.03	67	22	50	18
240, CD	0.66 ± 0.03	0.43 ± 0.04	135	19.1	220	31
240, CE	0.64 ± 0.04	0.18 ± 0.02	8920	135	78	83
360, CD	0.65 ± 0.05	0.42 ± 0.03	371	20.6	330	89
360, CE	0.67 ± 0.03	0.17 ± 0.03	68200	246	115	433
480, CD	0.68 ± 0.03	0.43 ± 0.03	678	22.2	404	170
480, CE	0.65 ± 0.04	0.20 ± 0.02	157000	432	136	779

From Fig. 4 one can see that all the quantities $\langle m_r^{(l,m,s)} \rangle$ are negligibly small in the isotropic phase I due to the absence of elongated objects. In the region II the values of all $\langle m_r^{(l,m,s)} \rangle$ appear to be much bigger than in the Flory state. This is consistent with visual observations where one sees local orientational ordering in some regions of the globule. Across the transition between phases II and III, the values of $\langle m_r^{(m,s)} \rangle$ fall to zero, while the value of $\langle m_r^{(l)} \rangle$ essentially increases. In the ideal case when one can neglect the noise, the quantity $\langle m_r^{(l)} \rangle$ scales with the degree of polymerization as,

$$\langle m_r^{(l)} \rangle \rightarrow N, \quad N \rightarrow \infty, \quad (7)$$

i.e., all chain segments come to be distributed in a rodlike manner if the surface effects are negligible.

IV. KINETIC CONSIDERATIONS

In this section we present results for kinetics at the transition from the Flory to the various collapsed states. The kinetic processes at the collapse transition into phase I (line AB in Fig. 1) in the present model have been investigated extensively in the research of Ref. 3 and kinetic laws during different kinetic stages have been obtained. Here we discuss the possible applicability of those laws to the new transitions just discussed. Thus we will present kinetics results for the rapid quenches Flory \rightarrow phase II (line CD in Fig. 1) and Flory \rightarrow phase III (line CE). Kinetics calculations for quenches across different collapsed phases are a significant computational task due to the large characteristic times of rearrangements in a dense globular state.

Consistent with previous calculations, during the earliest kinetic stages we find there is rapid formation of small locally compacted globules. A mode coupling mechanism for the internal modes leads to a decrease of the squared radius of gyration by a power law,³

$$\Delta R_g^2(t) = -At^\alpha, \quad \alpha = 7/11 \approx 0.636. \quad (8)$$

It is not yet clear if indeed this is the origin of the early stage law. The value of the exponent α obtained from simulations of the kinetics to the phase I is a little bigger $\alpha = 0.66 \pm 0.03$. Numerical values of the exponent α obtained from simulations of early-stage kinetics to the other collapsed states for

different degrees of polymerization are exhibited in Table I. One can see that the values of the exponent α for kinetics to different regions of the phase diagram are nearly the same. Thus, whatever the explanation, this early-stage results does indeed seem to be universal. Nevertheless, the internal structures of those locally collapsed globules obtained at early times as we pass to phases II and III are different and seem to be similar to the structure of the final collapsed state in equilibrium.

The second kinetic regime of the transition from Flory to the phase I proceeds mainly by unification of smaller clusters as we have earlier argued.³ It was established that clusters grow according to a power law,

$$S = N(t/\tau_S)^Z, \quad Z = 1/2, \quad (9)$$

where S is the average number of monomers in a cluster. We call the parameter τ_S the total collapse time. The evolution of the squared radius of gyration during that stage may also be approximated by a few terms of the series

$$R_g^2(t) = R_g^2(\infty) + \sum_{\alpha} A_{\alpha} \exp(-t/\tau_{\alpha}). \quad (10)$$

For convenience we arrange the relaxation times τ_{α} in decreasing order $\tau_{\alpha} \geq \tau_{\alpha'}$ for $\alpha < \alpha'$. We call the relaxation time τ_1 the characteristic collapse time. For kinetics $A \rightarrow B$ both characteristic and total collapse times scale with the degree of polymerization as $\tau \propto N^2$. The fact that τ_S and τ_1 have the same scaling with N is as one would expect from a continuous transition.

Our attempts to apply the middle kinetic stage laws (9) and (10) to the kinetics at other collapse transitions are presented in Table I. The typical evolutions of the squared radii of gyration R_g^2 during that kinetic stage for different kinetic processes are presented in Fig. 5. One can see that the relaxation processes in the phase III are very slow compared to those in other collapse regions. After small anisotropic globules have been created during the first kinetic stage, their further unification is inhibited due to different orientations in neighboring globules. Thus, for this case the final value of the squared radius of gyration $R_g^2(\infty)$ exhibited in Table I is still far enough from the one obtained from equilibrium calculations. Furthermore, the numerical values of the total col-

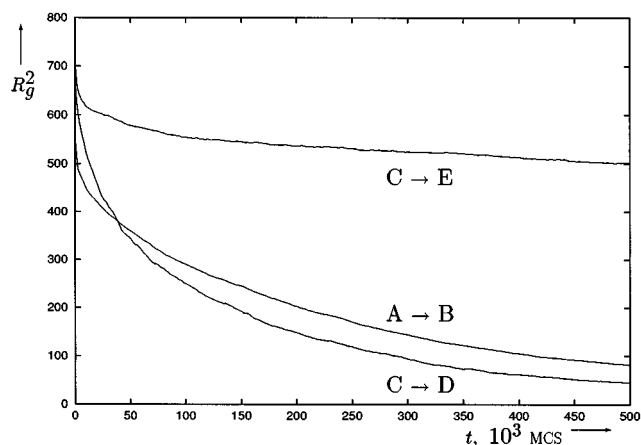


FIG. 5. Plots of the squared radius of gyration R_g^2 vs time t for polymer with the degree of polymerization $N=480$ for different collapse transitions. Labels denote the initial and final point in the phase diagram according with Fig. 1.

lapse times τ_S are very large. We must point out that this orientational frustration of locally collapsed globules is exacerbated by virtue of the underlying lattice. However, we expect this motif to persist even in continuum calculations.

On the contrary, the kinetic process in the phase II do not lead to metastable states. The reason seems to lie in the fact that the anisotropic accumulations are quite unstable in that region of the interaction parameters. Thus, some rearrangements of internal structure makes possible further unification of clusters. The simulation data appear to be consistent with the kinetic laws proposed earlier, but with new exponents. Without offering any theoretical interpretation we present them below,

$$\tau_1 \propto N^\gamma, \quad \gamma = 2.51 \pm 0.06 \approx 5/2,$$

$$\tau_S \propto N^{\gamma'}, \quad \gamma' = 2.32 \pm 0.05 \approx 7/3.$$

It is interesting to note that the characteristic and total collapse times [see Eqs. (9) and (10)] scale with the degree of polymerization in a different manner.

V. CONCLUSION AND DISCUSSIONS

In conclusion, then, we find that competition between local rigidity, expressed as a three-body repulsion, and pairwise attractions leads to three types of condensed state, one the conventional collapsed state, and the other two possessing orientational order to some degree. Although we recognize that the lattice may induce artefacts, we believe that the basic equilibrium picture is as argued in this paper. Thus, consider the limit of strongly repulsive three-body effects, and strongly attractive two-body interactions. It seems clear that the final state should be a bundle of aligned rigid rods arranged in a globular compacted state. This permits us to achieve the optimal condition for essentially all of the potential two-body interactions, and most of the three-body repulsions. The only unfavorable three-body interactions are those that occur at the surface of the globule, and they may therefore be expected to become less relevant in the long chain

limit. Packing forces also seem to be optimized by this arrangement. The only obvious breakdown of this rationale could arise if contour fluctuations destroyed this ordered structure. However, there appear to be no unquenched collective motions that could accomplish this. Such arguments rationalize the existence of phase III. Given this, it seems reasonable that there could exist one other, at least metastable, partially orientationally ordered structure. Thus, locally oriented clusters may join together with differing orientations, and given the connectivity constraints we can but expect at least a metastable arrangement of this type.

The distinction between the Flory and phase II is consistent with a type of glass transition, whilst that between I and III is consistent with crystallization, but the simulation data are not conclusive on this point.

We have also presented kinetic results but without theoretical interpretation. Possibly the differences in exponents we have found are significant enough to represent a fundamentally different mechanism from the conventional case of relaxation of an effective intermediate Gaussian coil.² It would be of considerable interest if this mechanism is a consequence of the transition being quite different. We may be beginning to see a complete set of analogues of the solid-liquid-gas transition kinetics that has been studied in the last twenty years, but this is a matter of further researches.

ACKNOWLEDGMENTS

The authors acknowledge interesting discussions with Professor K. Yoshikawa, Dr. A. Gorelov, and Dr. A. du Chesne. This work was supported by DEC and the Irish Government.

¹P. G. de Gennes, *Scaling Concepts in Polymer Physics* (Cornell University, Ithaca, NY, 1988), 3rd printing; M. Doi and S. F. Edwards, *The Theory of Polymer Dynamics* (Oxford Science, New York, 1989); J. des Cloizeaux and G. Jannink, *Polymers in Solution* (Clarendon, Oxford, 1990).

²P. G. de Gennes, *J. Phys. Lett.* **46**, L639 (1985); B. Ostrovsky and Y. Bar'Yam, *Comp. Polym. Sci.* **3**, 9 (1993); A. Byrne, P. Kiernan, D. Green, and K. A. Dawson, *J. Chem. Phys.* **102**, 573 (1995); E. G. Timoshenko and K. A. Dawson, *Phys. Rev. E* **51**, 492 (1995); E. G. Timoshenko, Yu. A. Kuznetsov, and K. A. Dawson, *J. Chem. Phys.* **102**, 1816 (1995).

³Yu. A. Kuznetsov, E. G. Timoshenko, and K. A. Dawson, *J. Chem. Phys.* **103** (11), 4807 (1995).

⁴S. M. Melnikov, V. G. Sergeyev, and K. Yoshikawa, Proceedings of International Conference "Nano-structures and Self-assemblies in Polymer Systems," St. Petersburg-Moscow, May 18-26 (1995); S. Kidoaki and K. Yoshikawa, Proceedings of International Conference "Nanostructures and Self-assemblies in Polymer Systems," St. Petersburg-Moscow, May 18-26 (1995).

⁵S. Fujishige, K. Kubota, and I. Ando, *J. Phys. Chem.* **93**, 3311 (1989); H. G. Schild, *Prog. Polym. Sci.* **17**, 163 (1992); A. V. Gorelov, L. N. Vasil'eva, A. Du Chesne, E. G. Timoshenko, Yu. A. Kuznetsov, and K. A. Dawson, *Nuovo Cimento* **16D**, 711 (1994).

⁶This particular choice of the two-body interaction function $w(r)$ is different from the one of Ref. 3. The phase diagram has the same structure in both cases, but the present choice makes the region II of the phase diagram more pronounced.

⁷*Monte Carlo Methods in Statistical Physics*, edited by K. Binder (Springer-Verlag, Berlin, 1986) 2nd ed.; *Applications of Monte Carlo Method in Statistical Physics*, edited by K. Binder (Springer-Verlag, Berlin, 1987), 2nd ed.; M. P. Allen and D. J. Tildesley, *Computer Simulations of Liquids* (Clarendon, Oxford, 1987); H. P. Witmann and K. Kremer, *Comput. Phys. Commun.* **61**, 309 (1990); M. A. Smith, Y. Bar-Yam, Y.

Rabin, B. Ostrovski, C. A. Bennett, N. Margolus, and T. Toffoli, *Comput. Polym. Sci.* **2**, 165 (1992).

⁸P. G. de Gennes and J. Prost, *The Physics of Liquid Crystals* (Clarendon, Oxford, 1993).

⁹We derive this formula as follows. The probability of a straight walk of length k along one of the axes x, y, z in some direction starting from an arbitrary point on the lattice is

$$P_k = \frac{6}{26} \left(\frac{1}{21}\right)^{k-1}.$$

Here the first multiplier represents the probability of the first step, and the

second of any further one. By definition, then, b can be written as

$$b = \sum_{k=3}^{\infty} k P_k.$$

Although this is obviously a quite rough estimate, it appears to be in fair agreement with (5).

¹⁰Our time unit, called Monte Carlo sweep (MCS), represents the sequence of N attempts to update the microscopic configuration of the system, where N is the degree of polymerization.